A Full-Wave Modal Analysis of Arbitrarily Shaped Waveguide Discontinuities Using the Finite Plane-Wave Series Expansion

Robert H. MacPhie, *Life Fellow, IEEE,* and Ke-Li Wu, *Senior Member, IEEE*

***Abstract*— A full-wave electromagnetic model for analyzing waveguide discontinuities of arbitrarily shaped piecewise planar boundaries is presented. The analysis is facilitated by using the finite plane-wave series expansion of circular cylindrical modal functions. Since electromagnetic fields on each of the planar boundary surfaces of the inhomogeneous region are expressed in terms of plane-wave modal functions, the complete solution is carried out analytically without any numerical integration. To verify the formulation, a number of practical waveguide components are analyzed. The calculated results are compared with other full-wave electromagnetic models. Excellent agreement is obtained for all the cases.**

***Index Terms*—Full-wave modal analysis, inhomgeneous waveguide junctions.**

I. Introduction

ELECTROMAGNETIC modeling of waveguide discontinuities with irregular shapes has drawn the attention of many researchers for decades [1] due to its wide application in microwave systems. The analysis methods for the waveguide discontinuities can be classified in two categories: the numerical or the analytical. The numerical ones, such as the finite-element method (FEM) [2], [3], boundary-element method (BEM) [4], or other hybrid techniques [5], in spite of their great advantages of flexibility and versatility, suffer from the errors of discretization and rounding off. On the other hand, the existing analytical methods are only applicable to the few regularly shaped waveguide discontinuities whose eigenmode functions can be solved analytically, such as waveguide T-junctions [6]. Although the segmentation method has been used in conjunction with modal analysis to solve some of the irregularly shaped discontinuities, e.g., mitered E-plane waveguide bend [7], since it still requires eigenmode functions for each divided subregion, very few nonregularly shaped waveguide discontinuities can take advantage of it. A power series solution of Maxwell's equations was also proposed to solve waveguide discontinuities of arbitrary shape; however, it has been found that some spurious solutions may occur in its eigen equation for higher order modes [8].

Manuscript received September 17, 1997.

R. H. MacPhie is with the Department of Electrical and Computer Engineering, University of Waterloo, Waterloo, Ont., Canada N2L 3G1.

K.-L. Wu is with the Corporate R&D Department, Com Dev, Cambridge, Ont., Canada N1R 7H5.

Publisher Item Identifier S 0018-9480(99)01144-8.

A general full-wave analysis of arbitrarily shaped waveguide discontinuities was reported by Reiter and Arndt in [9] using the boundary contour mode-matching method. The method can solve E- and H-plane waveguide discontinuities of virtually any shape. The significance of the work is that it formulates, for the first time, the problem with general cylindrical modal functions, representing the wave motion in all the directions. Unfortunately, since the Bessel–Fourier functions are involved in the field expression on the boundary of the inhomogeneous region, a numerical integration is needed to carry out the Galerkin solution procedure. The errors caused by the numerical integration may deteriorate the accuracy of the full-wave formulation.

In this paper, the general full-wave analysis is facilitated by using the finite plane-wave series expansion of the cylindrical Bessel–Fourier modal functions [10]. This work can be considered as an analytical extension of Reiter and Arndt's work [9]. The cylindrical modal functions are converted to a finite series of simple exponential plane-wave functions. Since electromagnetic fields on the piecewise planar boundary of the inhomogeneous region are expressed in terms of plane-wave modal functions, the complete solution is carried out analytically without any numerical integration. This feature retains the accuracy and efficiency of the full-wave solution.

This paper begins with the modal field expressions of the inhomogeneous region in terms of plane-wave functions. The detailed field-matching procedure is described. A number of practical waveguide components are analyzed both by the proposed analytical formulation and other numerical techniques. Excellent agreement is obtained for all the cases. It is worth mentioning that the original finite plane-wave series expansion has been extended to the cases where the radial argument of the cylindrical Bessel function is purely imaginary. This extension permits the use of all the possible modes existing in an inhomogeneous region of arbitrary shape.

II. Theoretical Formulations

A waveguide discontinuity of arbitrary shape can be modeled by an inhomogeneous cavity region having arbitrarily located planar sidewalls W_s and waveguide apertures or ports A_k, and with planar top and bottom walls located at $z = w$ and $z = 0$, respectively, as illustrated in Fig. 1. In this particular case, there are six sidewalls and three rectangular apertures, i.e., a rectangular waveguide three-port junction. As particular

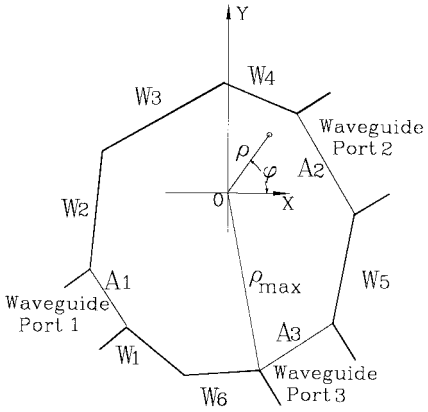

Fig. 1. An inhomogeneous waveguide discontinuity with planar sidewalls fed by rectangular waveguides through planar apertures A_k, with $s = 1, 2, \cdots, 6, k = 1, 2, 3$.

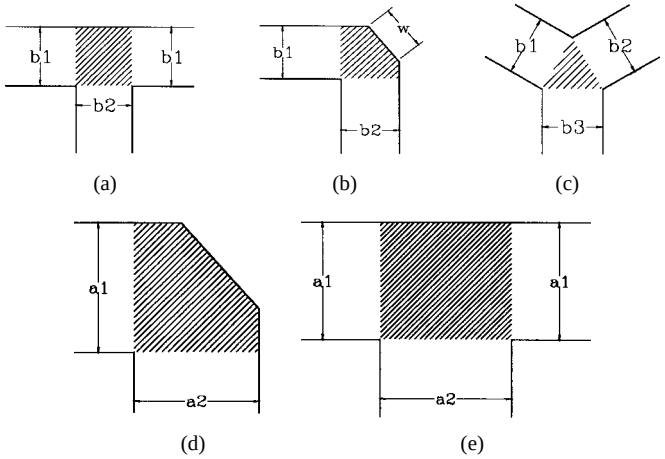

Fig. 2. Various inhomogeneous waveguide discontinuities. (a) E-plane T-junction. (b) E-plane mitered bend. (c) E-plane Y-junction. (d) H-plane mitered bend. (e) H-plane T-junction. The inhomogeneous region is cross-hatched.

examples of such inhomogeneous regions, Fig. 2 shows E- and H-plane T-junctions, an E-plane Y-junction, and E- and H-plane mitered bends. In each case, the inhomogeneous region is cross-hatched.

Modal Functions in the Inhomogeneous Region

To represent the electromagnetic fields in the various inhomogeneous regions, short circuited at $z = 0$ and w, but with quite arbitrary sidewalls and apertures, we can use the h- and e-type Bessel–Fourier modal potential functions, which have been introduced in [9]

$$\psi_{\substack{c\\snp}}^{(h)}(\rho,\phi,z) = J_n(h_n\rho)\begin{Bmatrix}\cos(n\phi)\\ \sin(n\phi)\end{Bmatrix}\sin\left(\frac{p\pi}{w}\,z\right) \quad (1)$$

$$\psi_{\substack{c\\snp}}^{(e)}(\rho,\phi,z) = J_n(h_n\rho)\begin{Bmatrix}\cos(n\phi)\\ \sin(n\phi)\end{Bmatrix}\cos\left(\frac{p\pi}{w}\,z\right). \quad (2)$$

From (1) and (2), one obtains, respectively, the modal E- and H- fields

$$\vec{e}_{\substack{c\\snp}}^{(h)} = -\nabla\times\hat{z}\psi_{\substack{c\\snp}}^{(h)} \quad (3)$$

$$\vec{h}_{\substack{c\\snp}}^{(h)} = \nabla\times\hat{z}\psi_{\substack{c\\snp}}^{(e)}. \quad (4)$$

The origin of the circular cylindrical coordinate is located centrally within the inhomogeneous region (see Fig. 1). In both cases, we have

$$h_p^2 = k^2 - \left(\frac{p\pi}{w}\right)^2 \quad (5)$$

where $k = \sqrt{\mu\varepsilon}$ is the wavenumber in the inhomogeneous region. Using (1) in (3), we obtain the h-type electric modal field

$$\vec{e}_{\substack{c\\snp}}^{(h)}(\rho,\phi,z) = \left[\frac{nJ_n(h_p\rho)}{\rho}\begin{pmatrix}\sin(n\phi)\\ -\cos(n\phi)\end{pmatrix}\hat{\rho} + h_\rho J_n'(h_p\rho)\begin{pmatrix}\cos(n\phi)\\ \sin(n\phi)\end{pmatrix}\hat{\phi}\right]\sin\left(\frac{p\pi}{w}\,z\right) \quad (6)$$

and the associated magnetic field is obtained from Maxwell's equations

$$\vec{h}_{\substack{c\\snp}}^{(h)}(\rho,\phi,z) = \frac{-1}{j\omega\mu_0}\cdot\left\{\begin{array}{l} -\dfrac{p\pi}{w}\,h_\rho J_n'(h_\rho\rho)\begin{pmatrix}\cos(n\phi)\\ \sin(n\phi)\end{pmatrix}\cos\left(\dfrac{p\pi}{w}\,z\right)\hat{\rho}\\ \quad +\dfrac{p\pi}{w}\,\dfrac{nJ_n(h_p\rho)}{\rho}\begin{pmatrix}\sin(n\phi)\\ -\cos(n\phi)\end{pmatrix}\cos\left(\dfrac{p\pi}{w}\,z\right)\hat{\phi}\\ \quad -h_p^2 J_n(h_p\rho)\begin{pmatrix}\cos(n\phi)\\ \sin(n\phi)\end{pmatrix}\sin\left(\dfrac{p\pi}{w}\,z\right)\hat{z}\end{array}\right\}. \quad (7)$$

Similar field expressions can be obtained for the e-type modes using (2) and (4).

However, because of the planar nature of the boundary walls W_s and boundary apertures A_k of the inhomogeneous region, circular cylindrical coordinates are not convenient for the task of analytically satisfying the electromagnetic boundary conditions on W_s and A_k. This problem is addressed in the following section.

Plane-Wave Expansion of the Circular Cylindrical Mode Functions in the Inhomogeneous Region

We wish to convert the electric- and magnetic-mode functions, as given by (6) and (7), from circular cylindrical coordinates (ρ,ϕ,z) to rectangular (x,y,z) coordinates. In the analysis of scattering at large circular to small rectangular waveguide junctions [10], the authors have shown that the h-type modal E-field, as given in circular cylindrical coordinates by (6), can be represented by a finite series of plane wave in rectangular coordinates

$$\vec{e}_{\substack{c\\snp}}^{(h)}(\rho,\phi,z) = h_p j^{n+1}\,\frac{1}{N}\sum_{l=0}^{N-1}[\hat{x}S_l - \hat{y}C_l]\cdot\begin{pmatrix}C_{ln}\\ S_{ln}\end{pmatrix}e^{-jh_p(C_lx+S_ly)}\sin\left(\frac{p\pi}{w}\,z\right) \quad (8)$$

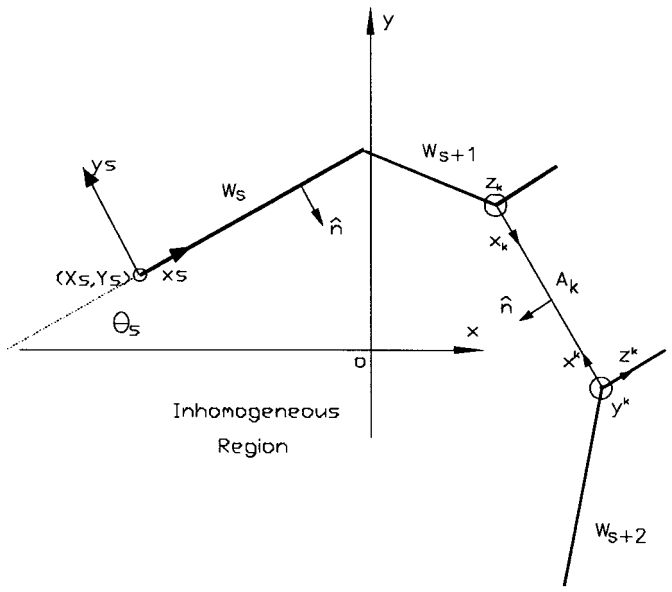

Fig. 3. The coordinate system of the conducting wall W_s and waveguide port with aperture A_k.

where

$$C_l = \cos\left(\frac{l2\pi}{N}\right)$$
$$S_l = \sin\left(\frac{l2\pi}{N}\right)$$
$$C_{ln} = \cos\left(\frac{ln2\pi}{N}\right)$$

and

$$S_{ln} = \sin\left(\frac{ln2\pi}{N}\right).$$

As described in [10], the number of terms N in the plane-wave series is determined by the inequality of

$$h_p \rho_{\max} < \frac{N-1}{2} - N_0$$

where relaxation constant N_0 is a small integer and $\rho_{\max}$ is the inhomogeneous region's maximum radial dimension (see Fig. 1).

Now, for field matching on the planar side wall W_s, we define a coordinate system (x_s, y_s, z_s) whose origin (see Fig. 3) is at $(x, y, z) = (X_s, Y_s, 0)$. With y_s perpendicular to W_s, which is at an angle θ_s with respect to the x-axis, we find that

$$\hat{x}_s = \cos\theta_s \hat{x} + \sin\ \theta_s \hat{y} = C_x \hat{x} + S_s \hat{y} \tag{9}$$
$$\hat{y}_s = S_x \hat{x} - C_s \hat{y}, \quad \hat{z}_s = \hat{z} \tag{10}$$

and

$$x = X_s + C_s x_s - S_s y_s, \quad y = Y_s + S_s x_s + C_s y_s \quad z = z_s. \tag{11}$$

By taking the scalar product of (8) with $\hat{x}_s$ and using (9)–(11), we obtain

$$e^{(h)}_{c_{snp\,x_s}}(x_s, y_s, z_s) = h_p j^{n+1} \frac{1}{N} \sum_{l=0}^{N-1} S_{ls} \begin{pmatrix} C_{ln} \\ S_{ln} \end{pmatrix} e^{-jh_p(C_l X_s + S_l Y_s)} \cdot e^{-jh_p(C_{ls} x_s + S_{ls} y_s)} \sin\left(\frac{p\pi}{w} z_s\right) \tag{12}$$

with

$$S_{ls} = \sin\left(\frac{l2\pi}{N} - \theta_s\right) \quad \text{and} \quad C_{ls} = \cos\left(\frac{l2\pi}{N} - \theta_s\right). \tag{13}$$

Consequently, the n-pth h-type tangential E-field on the inhomogeneous-region boundary wall W_s is obtained by setting $y_s = 0$ in (12). Using the same transformation technique, we can obtain the x_s and z_s components of all the E- and H-field mode functions of h- and e-type. For the sake of completeness, we list them below.

For TE modes,

$$e^{(h)}_{c_{snp\,x_s}}(x_s, z_s) = A_{pn} \sum_{l=0}^{N-1} S_{ls} \begin{pmatrix} C_{ln} \\ S_{ln} \end{pmatrix} \cdot E_{pls} e^{-jh_p(C_{ls} x_s)} \sin\left(\frac{p\pi}{w} z_s\right) \tag{14a}$$

$$h^{(h)}_{c_{snp\,x_s}}(x_s, z_s) = \frac{-(p\pi/w)}{j\omega\mu_0} A_{pn} \sum_{l=0}^{N-1} C_{ls} \begin{pmatrix} C_{ln} \\ S_{ln} \end{pmatrix} \cdot E_{pls} e^{-jh_p(C_{ls} x_s)} \cos\left(\frac{p\pi}{w} z_s\right) \tag{14b}$$

$$h^{(h)}_{c_{snp\,z_s}}(x_s, z_s) = \frac{h_p}{j\omega\mu_0} \frac{1}{j} A_{pn} \sum_{l=0}^{N-1} \begin{pmatrix} C_{ln} \\ S_{ln} \end{pmatrix} \cdot E_{pls} e^{-jh_p(C_{ls} x_s)} \sin\left(\frac{p\pi}{w} z_s\right) \tag{14c}$$

and for TM modes,

$$e^{(e)}_{c_{snp\,x_s}}(x_s, z_s) = \frac{(p\pi/w)}{j\omega\varepsilon_0} A_{pn} \sum_{l=0}^{N-1} C_{ls} \begin{pmatrix} C_{ln} \\ S_{ln} \end{pmatrix} \cdot E_{pls} e^{-jh_p(C_{ls} x_s)} \sin\left(\frac{p\pi}{w} z_s\right) \tag{14d}$$

$$e^{(e)}_{c_{snp\,z_s}}(x_s, z_s) = \frac{h_p}{j\omega\varepsilon_0} \frac{1}{j} A_{pn} \sum_{l=0}^{N-1} \begin{pmatrix} C_{ln} \\ S_{ln} \end{pmatrix} \cdot E_{pls} e^{-jh_p(C_{ls} x_s)} \cos\left(\frac{p\pi}{w} z_s\right) \tag{14e}$$

$$h^{(e)}_{c_{snp\,x_s}}(x_s, z_s) = -A_{pn} \sum_{l=0}^{N-1} S_{ls} \begin{pmatrix} C_{ln} \\ S_{ln} \end{pmatrix} \cdot E_{pls} e^{-jh_p(C_{ls} x_s)} \cos\left(\frac{p\pi}{w} z_s\right) \tag{14f}$$

where $A_{pn} = j^{n+1}(h_p/N)$ and $E_{pls} = e^{-jh_p(C_l X_s + S_l Y_s)}$ are constant.

It should be mentioned that these plane-wave expression are valid even if $h_p = \sqrt{k^2 - (p\pi/w)^2}$ is pure imaginary, which occurs when $k < (p\pi/w)$.

The Fields-Matching Procedure

The inhomogeneous waveguide region can be considered as a section of homogeneous waveguide in the z-direction. The total electric and magnetic fields are simply the superposition of the TE and TM modes with respect to the z-direction. Specifically, the total tangential fields on the boundary Γ can be expressed as

$$\vec{E}_{i\Gamma} = \sum_q (\alpha_q^h \vec{e}_q^h + \alpha_q^e \vec{e}_q^e)$$

and

$$\vec{H}_{i\Gamma} = \sum_q (\alpha_q^h \vec{h}_q^h + \alpha_h^e \vec{h}_q^e). \tag{15}$$

Here, the α_q are the weighting coefficients of each of the mode fields in the inhomogeneous region, which are defined in (14); q is a combined mode index $q = (n,p)$.

In each of the waveguide apertures A_k, $k = 1,2,\cdots,K$ the tangential electromagnetic fields must be continuous. We represent the rectangular waveguide fields by the traditional set of TE and TM modes. For example, at waveguide port k with rectangular coordinates (x_k, y_k, z_k),

$$\vec{E}_t^k = \sum_r (a_{rk}^h + b_{rk}^h)\sqrt{Z_{rk}^h}\,\vec{e}_{rk}^h + \sum_r (a_{rk}^e + b_{rk}^e)\sqrt{Z_{rk}^e}\,\vec{e}_{rk}^e, \tag{16a}$$

$$\vec{H}_t^k = \sum_r (-a_{rk}^k + b_{rk}^h)\frac{1}{\sqrt{Z_{rk}^k}}(\hat{z}^k \times \vec{e}_{rk}^h) + \sum_r (-a_{rk}^e + b_{rk}^e)\frac{1}{\sqrt{Z_{rk}^e}}(\hat{z}^k \times \vec{e}_{rk}^e) \tag{16b}$$

where $r = (\overline{m},\overline{n})$ is the combined-mode index, Z is the wave impedance of the corresponding mode, and a and b are the mode coefficients for the incident and reflected waves, respectively. The mode functions in rectangular waveguide k can be expressed as

$$\vec{e}_{rk}^h = A_{\overline{m}\,\overline{n}}^h \left\{ \hat{x}^k \left(\frac{\overline{m}\pi}{A_k}\right) \cos\left(\frac{\overline{m}\pi}{A_k}\,x^k\right) \sin\left(\frac{\overline{n}\pi}{w}\,y^k\right) - \hat{y}^k \left(\frac{\overline{n}\pi}{w}\right) \sin\left(\frac{\overline{m}\pi}{A_k}\,x^k\right) \cos\left(\frac{\overline{n}\pi}{w}\,y^k\right) \right\} \tag{17a}$$

$$\vec{e}_{rk}^e = A_{\overline{m}\,\overline{n}}^e \left\{ \hat{x}^k \left(\frac{\overline{m}\pi}{A_k}\right) \cos\left(\frac{\overline{m}\pi}{A_k}\,x^k\right) \sin\left(\frac{\overline{n}\pi}{w}\,y^k\right) - \hat{y}^k \left(\frac{\overline{n}\pi}{w}\right) \sin\left(\frac{\overline{m}\pi}{A_k}\,x^k\right) \cos\left(\frac{\overline{n}\pi}{w}\,y^k\right) \right\} \tag{17b}$$

where (x^k, y^k, z^k) are the local coordinates of the kth waveguide.

The boundary conditions on the waveguide ports and conducting walls need to be imposed to solve the waveguide discontinuity problem

$$\vec{E}_{i\Gamma} = \begin{cases} \vec{E}_t^k, & \Gamma = A_k \\ 0, & \text{elsewhere} \end{cases} \tag{18a}$$

$$\vec{H}_{i\Gamma} = \vec{H}_t^k, \qquad \Gamma = A_k. \tag{18b}$$

By taking outer products of (18a) on both sides with $\vec{h}_l^h$ and $\vec{h}_l^e$, respectively, to enforce the electric-field continuity condition, we have (19), shown at the bottom of this page, where the outer products are defined as

$$\langle \vec{e}_q^{\,(h)}_{(e)}, \vec{h}_l^{\,(h)}_{(e)} \rangle = \iint_\Gamma \vec{e}_q^{\,(h)}_{(e)} \times \vec{h}_l^{\,(h)}_{(e)} \cdot \hat{n}\, ds \tag{20a}$$

where $\Gamma = A + W$ is the total transverse surface of the inhomogeneous region with K apertures and S sidewalls.

Moreover,

$$\langle \sqrt{Z_{rk}^{(h)}_{(e)}}\,\vec{e}_{rk}^{\,(h)}_{(e)}, \vec{h}_l^{\,(h)}_{(e)} \rangle = \sqrt{Z_{rk}^{(h)}_{(e)}} \iint_{A_k} \vec{e}_{rk}^{\,(h)}_{(e)} \times \vec{h}_l^{\,(h)}_{(e)} \cdot \hat{n}\, ds. \tag{20b}$$

Next, by taking the outer products of (18b) on both sides with $\vec{e}_{lk}^h$ and $\vec{h}_{lk}^e$, respectively, to enforce the magnetic-field continuity condition, we have, due to mode orthogonality in the waveguides,

$$\begin{Bmatrix} a_{l1}^h - b_{l1}^h \\ a_{l1}^e - b_{l1}^e \\ \vdots \\ a_{lK}^h - b_{lK}^h \\ a_{lK}^e - b_{lK}^e \end{Bmatrix} = \underbrace{\begin{bmatrix} \langle \sqrt{Z_{l1}^h}\,\vec{e}_{l1}^h, \vec{h}_q^h \rangle & \langle \sqrt{Z_{l1}^h}\,\vec{e}_{l1}^h, \vec{h}_q^e \rangle \\ \langle \sqrt{Z_{l1}^e}\,\vec{e}_{l1}^e, \vec{h}_q^h \rangle & \langle \sqrt{Z_{l1}^e}\,\vec{e}_{l1}^e, \vec{h}_q^e \rangle \\ \cdots & \\ \langle \sqrt{Z_{lK}^h}\,\vec{e}_{lK}^h, \vec{h}_q^h \rangle & \langle \sqrt{Z_{lK}^h}\,\vec{e}_{lK}^h, \vec{h}_q^e \rangle \\ \langle \sqrt{Z_{lK}^e}\,\vec{e}_{lK}^e, \vec{h}_q^h \rangle & \langle \sqrt{Z_{lK}^e}\,\vec{e}_{lK}^e, \vec{h}_q^e \rangle \end{bmatrix}}_{[E]^T} \cdot \begin{Bmatrix} \alpha_q^h \\ \alpha_q^e \end{Bmatrix}. \tag{21}$$

By eliminating

$$\begin{Bmatrix} \alpha_q^h \\ \alpha_q^e \end{Bmatrix}$$

$$\underbrace{\begin{bmatrix} \langle \vec{e}_q^h, \vec{h}_l^h \rangle & \langle [\vec{e}_q^e, \vec{h}_l^h \rangle \\ \langle \vec{e}_q^h, \vec{h}_l^e \rangle & \langle [\vec{e}_q^e, \vec{h}_l^e \rangle \end{bmatrix}}_{[D]} \begin{Bmatrix} \alpha_q^h \\ \alpha_q^e \end{Bmatrix} = \underbrace{\begin{bmatrix} \langle \sqrt{Z_{r1}^h}\,\vec{e}_{r1}^h, \vec{h}_l^h \rangle \langle \sqrt{Z_{r1}^e}\,\vec{e}_{r1}^e, \vec{h}_l^h \rangle \cdots \langle \sqrt{Z_{rk}^h}\,\vec{e}_{rK}^h, \vec{h}_l^h \rangle \langle \sqrt{Z_{rK}^e}\,\vec{e}_{rK}^e, \vec{h}_l^h \rangle \\ \langle \sqrt{Z_{r1}^h}\,\vec{e}_{r1}^h, \vec{h}_l^e \rangle \langle \sqrt{Z_{r1}^e}\,\vec{e}_{r1}^e, \vec{h}_l^e \rangle \cdots \langle \sqrt{Z_{rk}^h}\,\vec{e}_{rK}^h, \vec{h}_l^e \rangle \langle \sqrt{Z_{rK}^e}\,\vec{e}_{rK}^e, \vec{h}_l^e \rangle \end{bmatrix}}_{[E]} \begin{Bmatrix} a_{r1}^h + b_{r1}^h \\ a_{r1}^e + b_{r1}^e \\ \cdots \\ a_{rK}^h + b_{rK}^h \\ a_{rK}^e + b_{rK}^e \end{Bmatrix} \tag{19}$$

from (19) and (21), we obtain

$$\begin{Bmatrix} a_{l1}^h - b_{l1}^h \\ a_{l1}^e - b_{l1}^e \\ \vdots \\ a_{lK}^h - b_{lK}^h \\ a_{lK}^e - b_{lK}^e \end{Bmatrix} = [E]^T[D]^{-1}[E] \begin{Bmatrix} a_{l1}^h + b_{l1}^k \\ a_{l1}^e + b_{l1}^e \\ \vdots \\ a_{lK}^h + b_{lK}^h \\ a_{lK}^e + b_{lK}^e \end{Bmatrix}$$

$$= [C] \begin{Bmatrix} a_{l1}^h + b_{l1}^h \\ a_{l1}^e + b_{l1}^e \\ \vdots \\ a_{lK}^h + b_{lK}^h \\ a_{lK}^e + b_{lK}^e \end{Bmatrix} \tag{22}$$

or

$$\{\boldsymbol{b}\} = [I + C]^{-1}[I - C]\{\boldsymbol{a}\} = [S]\{\boldsymbol{a}\} \tag{23}$$

where I is the identity matrix, $\{\boldsymbol{a}\}$ and $\{\boldsymbol{b}\}$ are the column vectors of incident and reflected rectangular waveguide amplitudes, and $[S]$ is the general scattering matrix of the waveguide discontinuity. It is worth mentioning that because of the use of the plane-wave series expansion on the planar matching surfaces of A_k and W_s, all the matrix elements in the above equations can be analytically evaluated. No numerical integration is required in the formulation. This feature is very important to retain the accuracy and efficiency of the analysis. Although, in the analysis, the height of each waveguide ports is the same as that of the inhomogeneous region, the formulation does not lose any generality since the field variation of the higher order modes in the height direction has been taken into account.

III. Numerical Results

A general full-wave analysis computer-aided design (CAD) program has been developed based on the theory of the finite plane-wave series expansion. In all the calculations, the relaxation constant is set to seven. It is worth mentioning that to improve the numerical condition of the matrix $[D]$, an appropriate normalization process needs to be applied in calculating (20a). To validate the theory, the five waveguide components, shown in Fig. 2, have been analyzed using the plane-wave expansion theory and are compared with other analytical and numerical methods. A very good agreement can be observed for all the cases.

WR75 Waveguide T-junctions of the E- and H-plane types are considered first. The waveguide dimensions are $a = 0.75''$ and $b = 0.375.''$ The T-junctions are also analyzed by conventional mode-matching techniques using rectangular waveguide eigenmode expansion [6]. Figs. 4 and 5 show the magnitudes of some typical scattering parameters of the E- and H-plane waveguide T-junctions, respectively, calculated by the formulation using plane-wave expansion and by the conventional mode-matching technique. It can be seen that the correlation is excellent.

A WR75 E-plane Y-junction has been taken as another example for the three-port waveguide component. The magnitudes of scattering parameters calculated by the plane-wave expansion theory and those by the full-wave BEM [4] are superposed in Fig. 6. Excellent agreement can be observed.

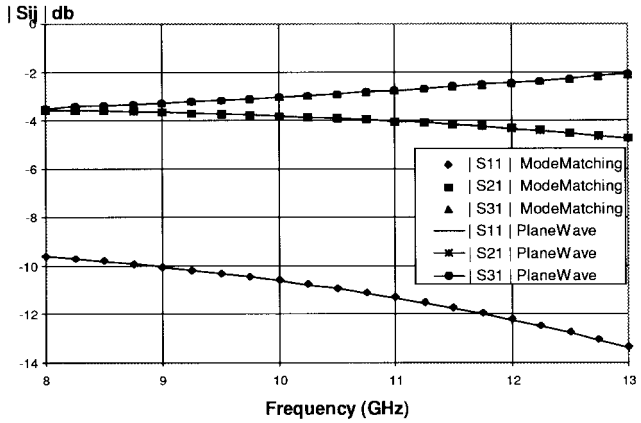

Fig. 4. The magnitude of scattering parameters or a WR75 waveguide E-plane T-junction with $a = 0.75$ in, $b1 = b2 = b3 = 0.375$ in.

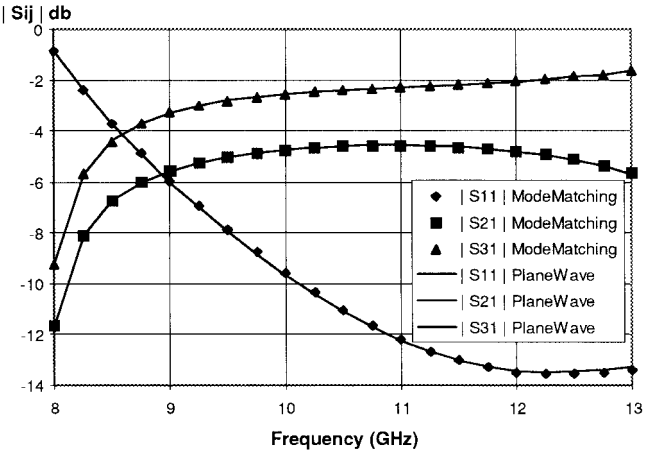

Fig. 5. The magnitude of scattering parameters for the WR75 waveguide H-plane T-junction with $a1 = a2 = a3 = 0.75$ in, $b = 0.375$ in.

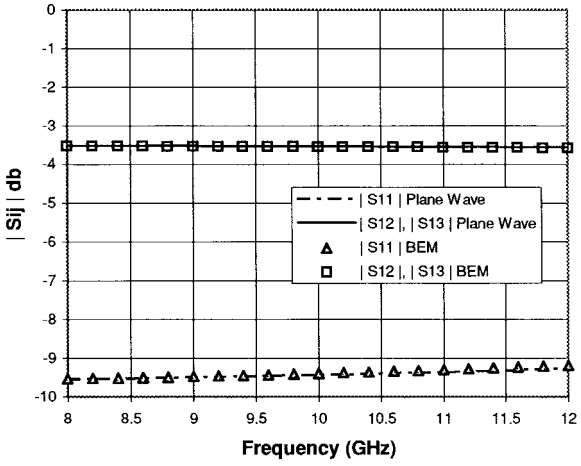

Fig. 6. The magnitude of scattering parameters of a WR75 waveguide E-plane Y-junction with $a = 0.75$ in, $b1 = b2 = b3 = 0.375$ in.

Although the waveguide mitered bend is one of the most commonly used waveguide components, there is no analytical CAD model available so far for its practical design. For software verification, both H- and E-plane WR75 mitered bends were designed using the formulation of plane-wave

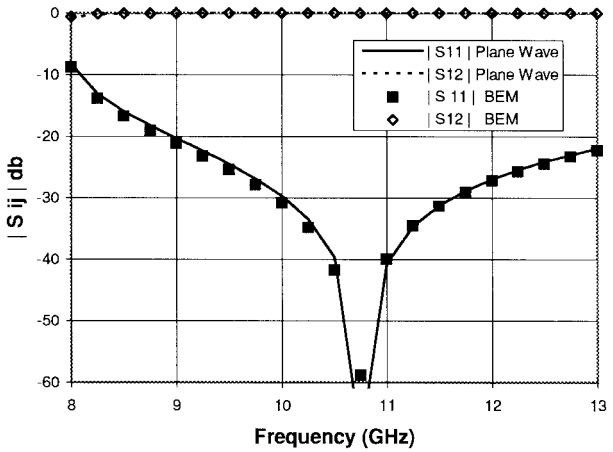

Fig. 7. The magnitude of scattering parameters of a WR75 H-plane mitered bend with $a = 0.75$ in, $b1 = b2 = 0.375$ in, and $W = 0.7266$ in.

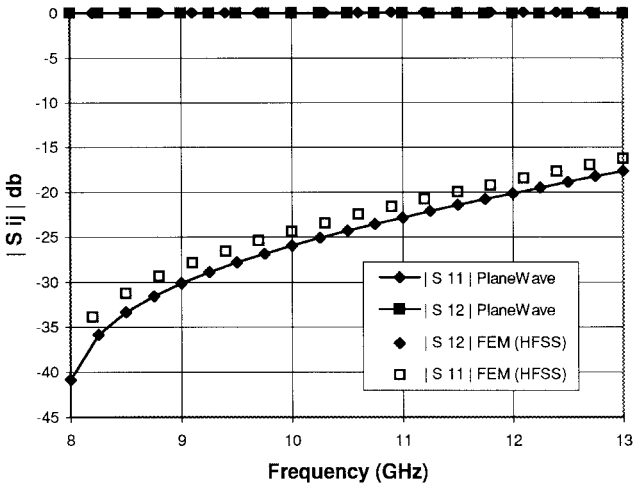

Fig. 8. The magnitudes of scattering parameters of a WR75 waveguide E-plane mitered bend with $a = 0.75$ in, $b1 = b2 = 0.375$ in, and $W = 0.4746$ in.

expansion. As shown in Fig. 7, the designed H-plane mitered bend has been verified by the results calculated using the BEM. As another independent verification, the analysis of an E-plane WR75 mitered bend using the plane-wave expansion has been verified by the full-wave FEM software package *eminence* developed by Ansoft corporation. As shown in Fig. 8, a good agreement is also obtained.

IV. Conclusions

This paper presented an analytical full-wave electromagnetic model for rectangular waveguide discontinuities of arbitrary shape. The finite plane-wave series expansion is used to facilitate the full-wave analysis. The analytical expressions for the elements of the field-matching matrix retain the accuracy and efficiency of the full-wave model. To validate the formulation, a number of practical waveguide components are analyzed. The calculated results are compared with other full-wave electromagnetic models. Excellent agreement is obtained for all the cases.

Although only the formulation for the piecewise planar boundaries are presented in the paper, the formulation can easily be extended to the cases with the boundary consisting of planar surfaces and segments of circular cylinders.

References

[1] N. Marcuvitz, *Waveguide Handbook*. New York: Dover, 1965.
[2] M. Koshiba and M. Suzuki, "Finite-element analysis of H-plane waveguide junction with arbitrarily shaped ferrite post," *IEEE Trans. Microwave Theory Tech.*, vol. MTT-34, pp. 103–109, Jan. 1986.
[3] J. P. Webb and S. Porihar, "Finite element analysis of H-plane rectangular waveguide problems," *Proc. Inst. Elect. Eng.*, vol. 133, pt. H, no. 2, pp. 91–94, Apr. 1986.
[4] M. Koshiba and M. Suzuki, "Application of the boundary-element method to waveguide discontinuities," *IEEE Trans. Microwave Theory Tech.*, vol. MTT-34, pp. 301–307, Feb. 1986.
[5] K.-L. Wu, G. Y. Delisle, D. G. Fang, and M. Lecours, "Waveguide discontinuities analysis with a coupled finite boundary-element method," *IEEE Trans. Microwave Theory Tech.*, vol. MTT-37, pp. 993–998, June 1989.
[6] E. Kuhn, "A mode-matching method for solving field problems in waveguide and resonator circuits," *AEU*, no. 12, pp. 511–518, 1973.
[7] F. Alessandri, M. Mongiardo, and R. Sorrentino, "Rigorous mode matching analysis of mitered E-plane bends in rectangular waveguide," *IEEE Microwave Guided Wave Lett.*, vol. 4, pp. 408–410, Dec. 1994.
[8] A. Morini and T. Rozzi, "Power series solution of Maxwell's equations of arbitrary shaped hollow waveguides," in *Proc. 26th EuMC*, 1996, pp. 722–725.
[9] J. M. Reiter and F. Arndt, "Rigorous analysis of arbitrarily shaped H- and E-plane discontinuities in rectangular waveguide by a full-wave boundary contour mode-matching method," *IEEE Trans. Microwave Theory Tech.*, vol. 43, pp. 796–801, Apr. 1995.
[10] R. H. MacPhie and K.-L. Wu, "Scattering at the junction of a rectangular waveguide and a large circular waveguide," *IEEE Trans. Microwave Theory Tech.*, vol. 43, pp. 2041–2045, Sept. 1995.

Robert H. MacPhie (S'57–M'63–SM'79–F'91–LF'97) was born in Weston, Ont., Canada, on September 20, 1934. He received the B.A.Sc. degree in electrical engineering from the University of Toronto, Toronto, Ont., Canada, in 1957, and the M.S. and Ph.D. degrees from the University of Illinois at Urbana-Champaign, in 1959 and 1963, respectively.

In 1963, he joined the University of Waterloo, Waterloo, Ont., Canada, as an Assistant Professor of electrical engineering, and is currently an Adjunct Professor of electrical and computer engineering. His current research interests focus on waveguide scattering theory, scattering from spherical systems, and dipole antennas. From 1991 to 1992, he was on sabbatical leave as a Professeur Associe in the Departement de Radioelectricite, University of Aix-Marseille 1, France.

Ke-Li Wu (M'90–SM'96) received the B.S. and M.S.E. degree from the East China Institute of Technology, China, in 1982 and 1985, respectively, and the Ph.D. degree from Laval University, Quebec, P.Q., Canada, in 1989, all in electrical engineering.

From 1985 to 1986, he was a Research Assistant in the East China Institute of Technology. From 1989 to 1993, he was with the Communications Research Laboratory, McMaster University, as a Research Engineer, where his responsibilities included electromagnetic modeling and development of advanced integrated antennas. He joined Com Dev, Cambridge, Ont., Canada in March 1993, where he is a Senior Member of Technical Staff in the Corporate R&D Department. He also holds an appointment of Adjunct Associate Professor at McMaster University. He has published over 30 journal papers. He contributed to *Finite Element and Finite Difference Methods in Electromagnetics Scattering* (Amsterdam, The Netherlands: Elsevier, 1990), and to *Computational Electromagnetics* (Amsterdam, The Netherlands, North-Holland, 1991). His current research interests include all aspects of numerical methods in electromagnetics with emphasis on the analysis of waveguide systems and interconnections of integrated RF circuits.